New Model That Describes Adsorption of Laterally Interacting Gas Mixtures on Random Heterogeneous Surfaces. 2. Correlation of Complex Binary and Prediction of Multicomponent Adsorption Equilibria

Shaheen A. Al-Muhtaseb and James A. Ritter*

Department of Chemical Engineering, Swearingen Engineering Center, University of South Carolina, Columbia, South Carolina 29208

Received March 2, 1999. In Final Form: June 10, 1999

The model developed in part 1 of this series for correlating single component and rather ideal binary adsorption equilibria demonstrated a remarkable ability for correlating complex binary adsorption equilibria, including adsorption azeotropes and sigmoidal-shaped $x-y$ diagrams, using a single binary fitting parameter. This model was also extended successfully for predicting multicomponent adsorption equilibria on a heterogeneous adsorbent surface with a uniform distribution of Henry's law constant using single component adsorption isotherm parameters, along with one binary fitting parameter from each of the binary pairs in the multicomponent mixture. Overall, the results from this new model generally showed a marked improvement in the correlation of binary and prediction of multicomponent adsorption equilibria compared to that obtained with the multicomponent Langmuir model, which used only single component isotherm parameters, and compared to that obtained with two-dimensional fluid and loading ratio correlation models that also utilized binary fitting parameters.

Introduction

Multicomponent adsorption models are needed for the design, development, and operation of gas separation and purification processes. Efficient models that can describe different adsorption nonidealities, such as adsorption azeotropes and sigmoidal-shaped $x-y$ diagrams, are required for highly interacting systems to cover the wide variation of conditions that exist in different adsorption processes. These conditions may vary substantially during the operation of a cyclic pressure or thermal swing adsorption process. Therefore, these models should possess enough flexibility to predict any nonideal behavior that may occur at any composition and temperature.

Very few binary and multicomponent adsorption models can predict adsorption azeotropes and asymmetric $x-y$ diagrams. Zhou et al.[1] demonstrated that adsorption azeotropes cannot be predicted using the mixed-Langmuir or ideal adsorbed solution (IAS) models without modifications. However, the IAS model was successfully extended to the heterogeneous ideal adsorbed solution (HIAS) model[2], and in this form it predicted azeotropic behavior.[3−6] Talu also used a heterogeneous form of the nonideal adsorbed solution theory (NIAS) to predict azeotropes.[7] However, in general, it was shown that the IAS theory can introduce some serious errors in calculating multicomponent adsorption equilibria from pure component adsorption isotherms when the adsorbate sizes and degrees of adsorption heterogeneity differ substantially for different components.[8] Other models that are capable of predicting adsorption azeotropes are fairly complicated in their use and include the vacancy solution theory (VST),[9,10] a beta-function site distribution model,[11] a semiempirical spreading pressure dependent nonideal IAS model,[12] a modified Dubinin−Raduskevich model,[13] and a statistical thermodynamic modification to a Langmuir-type kinetic model.[14] However, two additional models, based on extensions of the mixed-Langmuir model, are much simpler to use and include analytic expressions that can be used for the direct correlation of adsorption azeotropes:[15,16] Sircar[15] integrated over a uniform distribution of Henry's law constants to obtain analytic expressions for mixed-gas adsorption that accounts for surface heterogeneity and, based on earlier work by Yang and co-workers,[17,18] Sircar's approach was extended by Ritter and Al-Muhtaseb[16] to also account for lateral interactions.

The effects of surface heterogeneity, different site distributions, and lateral interactions on adsorption equilibria have been studied by many investigators.[16−17,19−24] Some of these studies have shown that

* To whom all correspondences should be addressed. E-mail: ritter@engr.sc.edu.

(1) Zhou, C.; Hall, M.; Gasem, K.; Robinson, Jr., R. *Ind. Eng. Chem. Res.* **1994**, *33*, 1280.
(2) Myers, A.; Prausnitz, J. *AIChE J.* **1965**, *11*, 121.
(3) Valenzuela, D. Physical Adsorption on Energetically Heterogeneous Surfaces. Ph.D. Dissertation in Chemical Engineering, University of Pennsylvania, 1987.
(4) Valenzuela, D. P.; Myers, A. L.; Talu, O.; Zwiebel, I. *AIChE J.* **1988**, *34*, 397.
(5) O'Brien, J. Studies of Molecular Interaction Effects in Physical Adsorption on Heterogeneous Solid Surfaces. Ph.D. Dissertation in Chemical Engineering, University of Pennsylvania, 1986.
(6) Moon, H.; Tien, C. *Chem. Eng. Sci.* **1988**, *43*, 2967.
(7) Talu, O. Thermodynamics of Multicomponent Gas Adsorption Equilibria of Non-Ideal Mixtures. Ph.D. Dissertation in Chemical Engineering, Arizona State University, 1984.
(8) Sircar, S. *AIChE J.* **1995**, *41*, 1135.
(9) Cochran, T.; Kabel, R.; Danner, R. *AIChE J.* **1985**, *31*, 269.
(10) Talu, O.; Myers, A. *AIChE J.* **1988**, *34*, 1931.
(11) Ou, D. The effect of Surface Heterogeneity on Adsorption from Gas and Liquid Mixtures. Ph.D. Dissertation in Chemical Engineering, University of Pennsylvania, 1982.
(12) Talu, O.; Zwiebel, I. *AIChE J.* **1986**, *30*, 1263.
(13) Sundaram, N. *Langmuir* **1995**, *11*, 3223.
(14) Martinez, G. Towards a General Gas Adsorption Isotherm (Adsorption Equilibrium). Ph.D. Dissertation in Chemical Engineering, University of Toronto, Toronto, Canada, 1992.
(15) Sircar, S. *Ind. Eng. Chem. Res.* **1991**, *30*, 1032.
(16) Ritter, J. A.; Al-Muhtaseb, S. A. *Langmuir* **1998**, *14*, 6528−6538.
(17) Ritter, J.; Kapoor, A.; Yang, R. *J. Phys. Chem.* **1990**, *94*, 6785.
(18) Kapoor, A.; Ritter, J. A.; Yang, R. T. *Langmuir* **1990**, *6*, 660.
(19) Kaminski, R.; Monson, P. *AIChE J.* **1992**, *38*, 1979.

10.1021/la990242g CCC: $18.00
Published on Web 08/28/1999

surface heterogeneity imparts changes to the binary selectivity, and hence the occurrence of adsorption azeotropes, by altering the ratio of the component Henry's law constants and through excluded volume effects.[15,19−20] However, only the recent work by Ritter and Al-Muhtaseb,[16] in part 1 of this series, revealed the roles of surface heterogeneity and lateral interactions in the prediction of adsorption azeotropes and sigmoidal $x-y$ diagrams, including how the empirical binary fitting parameter can account for pore exclusion effects that have been shown to cause azeotropic behavior.[19,20] Part 1[16] also demonstrated that the new model was capable of correlating rather ideal binary data.

Therefore, the objective of part 2 of this series is to further demonstrate the potential of this new model for correlating complex binary adsorption equilibria, including adsorption azeotropes and sigmoidal $x-y$ diagrams, using a single binary fitting parameter. It is also extended for predicting multicomponent adsorption equilibria using only single component and binary fitting parameters. Strengths and weaknesses of this new model are exposed and discussed relative to the multicomponent Langmuir model,[25] which uses only single component isotherm parameters, and relative to a two-dimensional fluid model[26] and the loading ratio correlation,[27] which both use binary fitting parameters.

Theory

Correlation of Single Component and Binary Adsorption Equilibria. The Fowler and Guggenheim (FG) isotherm was extended to account for adsorbent surface heterogeneity using a uniform distribution of Henry's law constants on a random heterogeneous surface.[16] The expression for this heterogeneous form of the single component FG (HFG) adsorption isotherm model is given by

$$\theta = \frac{n}{m} = 1 - \frac{1}{2\sqrt{3}\sigma\Omega P}\ln\left[\frac{1+(b+\sqrt{3}\sigma)\Omega P}{1+(b-\sqrt{3}\sigma)\Omega P}\right] \quad (1)$$

where θ is the overall fractional surface coverage on a random heterogeneous surface, n is the amount adsorbed, m is the saturation limit, P is the pressure, and σ is the heterogeneity parameter which represents the span between the Henry's law constants corresponding to the low and high limits of adsorption energies.[16] b is the adsorption energy parameter, expressed as

$$b = b_0 \exp\left(\frac{\epsilon}{RT}\right) \quad (2)$$

where ϵ is the average adsorption energy, R is the universal gas constant, T is the absolute temperature, and b_0 is the preexponential factor. The lateral interaction parameter, Ω, is given by

$$\Omega = \exp\left(\frac{-z\omega}{\kappa T}\theta\right) = \exp(-\alpha\theta) \quad (3)$$

where κ is Boltzmann's constant, $z\omega$ is the total energy of the lateral interactions, and $\alpha = z\omega/\kappa T$. In the limits of σ and ω both approaching zero, eq 1 reduces to the familiar Langmuir (LM) adsorption isotherm

$$\theta = \frac{bP}{1+bP} \quad (4)$$

The expression for binary adsorption was derived in part 1 of this series[16] as

$$\theta_i = \frac{n_i}{m_i} = \frac{\sigma_i\beta_i^{(2)}P_i}{\sum_{j=1}^{2}\sigma_j\beta_j^{(2)}P_j}\left(1 + \frac{1+\sum_{j=1}^{2}(b_j - b_i\sigma_j/\sigma_i)\beta_j^{(2)}P_j}{2\sqrt{3}\sum_{j=1}^{2}\sigma_j\beta_j^{(2)}P_j}\ln\left[\frac{1+\sum_{j=1}^{2}(b_j-\sqrt{3}\sigma_j)\beta_j^{(2)}P_j}{1+\sum_{j=1}^{2}(b_j+\sqrt{3}\sigma_j)\beta_j^{(2)}P_j}\right]\right) \quad (5)$$

where θ_i, n_i, m_i, σ_i, and b_i are as defined above for single component i. The parameters m_i, b_{0i}, ϵ_i/R, and $z\omega_i/\kappa$ are obtained from correlating eqs 1−3 with experimental adsorption isotherm data of component i. $\beta_i^{(2)}$ is a binary lateral interaction term, which is given by[16]

$$\beta_i^{(2)} = \exp(-\alpha_i\theta_i - \alpha_{ij}\theta_j) \quad (6)$$

where $i \neq j$, and α_{ij} is expressed as

$$\alpha_{ij} = (k_{ij} - 1)\sqrt{\alpha_i\alpha_j} \quad (7)$$

k_{ij} ($=k_{ji}$) is a binary fitting parameter obtained by fitting eqs 5−7 to experimental binary adsorption equilibria. This single binary fitting parameter gives this model a remarkable flexibility to describe complex binary adsorption equilibria, such as adsorption azeotropes and sigmoidal-shaped $x-y$ diagrams, as shown in part 1 of this series.[16]

Very few models in the literature use a binary fitting parameter in their development.[1,12,26,27] The most successful of these models[1,12] require dealing with spreading pressures instead of equilibrium pressures, which eliminates the possibility of obtaining analytic expressions for the binary and multicomponent adsorption equilibria. Nevertheless, two other models, the two-dimensional fluid (2DF) model[26] and the loading ratio correlation (LRC),[27] used this binary fitting parameter approach with moderate success for modeling single and binary adsorption equilibria on an activated carbon fiber and molecular sieves, respectively, without the need for replacing the equilibrium pressure with the spreading pressure. Since these two models are similar in principle to the new model developed in this work, they are used here for comparing the efficacy of eqs 5−7.

The 2DF model assumes a four-site patch distribution for which the single component isotherm on each patch is given by[26]

$$\theta = \frac{n}{q_0} = \frac{\eta}{\eta_{\max}} = \frac{1}{\eta_{\max}}\sum_{m_p=1}^{4}\eta^{(m_p)}f^{(m_p)} \quad (8)$$

where q_0 is the monolayer saturation limit and treated as a fitting parameter. η is a dimensionless surface density of the adsorbed molecules, where $\eta_{\max}$ equals 0.907 for close-packed hard disks[26] and is fixed at this value and

(20) Kaminski, R.; Monson, P. *Langmuir* **1993**, *9*, 561.
(21) Steele, W. *J. Phys. Chem.* **1964**, *67*, 2016.
(22) Karavias, K.; Myers, A. *Chem. Eng. Sci.* **1992**, *47*, 1441.
(23) Russell, B.; LeVan, M. *Chem. Eng. Sci.* **1996**, *51*, 4025.
(24) Bakaev, V.; Steele, W. *Langmuir* **1996**, *12*, 6119.
(25) Markham, E. D.; Benton, A. F. *J. Am. Chem. Soc.* **1931**, *53*, 497.
(26) Nitta, T.; Yamaguchi, A.; Tokunaga, N.; Katayama, T. *J. Chem. Eng. Japan.* **1991**, *24* (3), 313.
(27) Yon, C. M.; Turnock, P. H. *AIChE Symp. Ser.* **1971**, *67* (117), 75.

represents the maximum monolayer limit of η. $f^{(m_p)}$ is the probability of the occurrence of patch m_p ($m_p = 1-4$), with its values given by {0.573, 0.317, 0.095, 0.015} for the four consecutive patches, respectively.[26] $\eta^{(m_p)}$ is the local surface density of the molecules adsorbed on patch m_p and is given by

$$\eta^{(m_p)} = K^{(m_p)}\phi P\left[1 + K^{(m_p)}\phi P \times \exp\left(-\left[\frac{3 - 2\eta^{(m_p)}}{(1 - \eta^{(m_p)})^2} - \frac{v}{\kappa T}\right]\eta^{(m_p)}\right)\right]^{-1} \quad (9)$$

ϕ is the fugacity coefficient at P and T (assumed in this work to equal unity in order to match it with the proposed model). v/κ is a lateral interaction parameter that can be determined from the Lennard-Jones potential parameters.[26] $K^{(m_p)}$ is the local Henry's law constant on patch m_p and is given by

$$\ln K^{(m_p)} = \ln A_0 - (1/2)\ln([1 + \gamma t^{(m_p)}]T/T_0) + [1 + \gamma t^{(m_p)}]\epsilon_0/\kappa T \quad (10)$$

T_0 is a reference temperature (=298.15 K), and $\ln A_0$, γ, and ϵ_0/κ are fitting parameters. $t^{(m_p)}$ is a dimensionless adsorption energy for patch m_p and is determined from using the four-point approximation of the Gaussian distribution function, along with the aforementioned $f^{(m_p)}$, which gives {0.2735, 0.8230, 1.3803, 1.9518} for the four consecutive patches, respectively.[26]

In a similar manner, the amount adsorbed of component i in a binary or multicomponent mixture is obtained from eq 8, with the local amounts adsorbed of component i on patch m_p calculated from the following extension of eq 9:[26]

$$\eta_i^{(m_p)} = K_i^{(m_p)}\phi_i P_i\left[1 + \sum_{j=1}^{M} K_j^{(m_p)}\phi_j P_j \exp\left(\frac{-\eta^{(m_p)}}{1 - \eta^{(m_p)}} - \left(\frac{2 - \eta^{(m_p)}}{(1 - \eta^{(m_p)})^2}\right)\left(\sum_{l=1}^{M}\frac{q_{0l}}{q_{0j}}\eta_l^{(m_p)}\right) + \sum_{l=1}^{M}\frac{v_{jl}}{\kappa T}\eta_l^{(m_p)}\right)\right]^{-1} \quad (11)$$

where $K_i^{(m_p)}$ is given by eq 10, and q_{0l} and q_{0j} are obtained from single component adsorption equilibria, $\eta^{(m_p)}$ is the summation of $\eta_j^{(m_p)}$, and M is the number of components in the mixture. v_{jl} is the mixed lateral interaction between components j and l and is given by[26]

$$v_{jl} = (1 - k_{jl})\sqrt{v_j v_l q_{0l}/q_{0j}} \quad (12)$$

where v_j and v_l are the single component lateral interactions. Because of the coupling of eqs 8 and 9 for single component adsorption, the 2DF model is implicit in both n and P. Therefore, obtaining the fitting parameters by regressing this model to the experimental data requires a tedious nested optimization procedure, i.e., iterating on the fitting parameters and $\eta^{(m_p)}$ simultaneously.

In contrast to the proposed and 2DF models, the use of interaction parameters in the LRC model[27] was designed to always serve in a correlative manner, regardless of the number of components. The single component form of the LRC equation is given by[27]

$$\theta = \frac{n}{m} = \frac{(kP)^{1/B}}{1 + (kP)^{1/B}} \quad (13)$$

where k is Henry's law constant and given by the following equivalent from eq 2:[27]

$$k = \exp(k_0 + k_1/T) \quad (14)$$

B equals $(B_0 + B_1/T)$, where m, k_0, k_1, B_0, and B_1 are fitting parameters. The multicomponent form of the LRC model is given by[27]

$$\theta_i = \frac{n_i}{m_i} = \frac{(k_i P_i/\eta_i)^{1/B_i}}{1 + \sum_{j=1}^{M}(k_j P_j/\eta_j)^{1/B_j}} \quad (15)$$

where m_i, k_i, and B_i are obtained from single component adsorption equilibria according to eq 13, and where the adsorbate−adsorbate lateral interaction parameter, η_i, is not only specific to each adsorbate and adsorbent pair, it is also dependent upon all other molecular species in the system.[27] Therefore, η_i is a pure correlation parameter for binary and multicomponent adsorption equilibria, and η_i values for different mixtures cannot be interrelated which eliminates the possibility of its use in a predictive manner. For comparison purposes only, the η_i's for binary mixtures are assumed here to be symmetric for the two components and given the notation k_{12} (=k_{21}), for convenience.

Extension of FG Isotherm Model for Multicomponent Adsorption on Homogeneous Surfaces. The FG adsorption isotherm model has been extended for multicomponent adsorption equilibria using different approaches.[28−31] A statistical mechanic approach, suggested by Fowler and Guggenheim,[32] is used here to derive these formulas giving the same main trend obtained from the kinetic approach.[31] The complete canonical potential function for the adsorbed phase is used here for estimating the chemical potentials and defined as[32]

$$Q = g(N_s, N_1, \ldots, N_M) \times a(T, N_1, \ldots, N_M) \quad (16)$$

where N_s and N_j are the total number of sites on the surface of the adsorbent and the number of sites occupied by molecules of type, j, respectively. g represents the number of ways of distributing the adsorbed molecules over the adsorption sites and is defined using the Stirling approximation, $\ln n! = n \ln n - n$, as

$$\ln g(N_s, N_1, \ldots, N_M) = N_s \ln N_s - \sum_{k=1}^{M} N_k \ln N_k - (N_s - \sum_{k=1}^{M} N_k)\ln(N_s - \sum_{k=1}^{M} N_k) \quad (17)$$

a is the partition function that describes the internal degrees of freedom of the adsorbed molecules, which is referred to the usual energy zero of the lowest internal state of the gaseous molecule at infinite separation. Thus,

(28) Temkin, M. I. *Russ. J. Phys. Chem.* **1941**, *15* (2), 296.
(29) Tovbin, Y. K. *Theor. Exp. Chem.* **1982**, *18* (4), 417.
(30) Tovbin, Y. K. *Russ. Kinet. Catal.* **1983**, *24* (2), 317.
(31) Tovbin, Y. K. *Prog. Surf. Sci.* **1990**, *34*, 1.
(32) Fowler, R.; Guggenheim, E. A. *Statistical Thermodynamics*; Cambridge University Press: Cambridge, U.K., 1952.

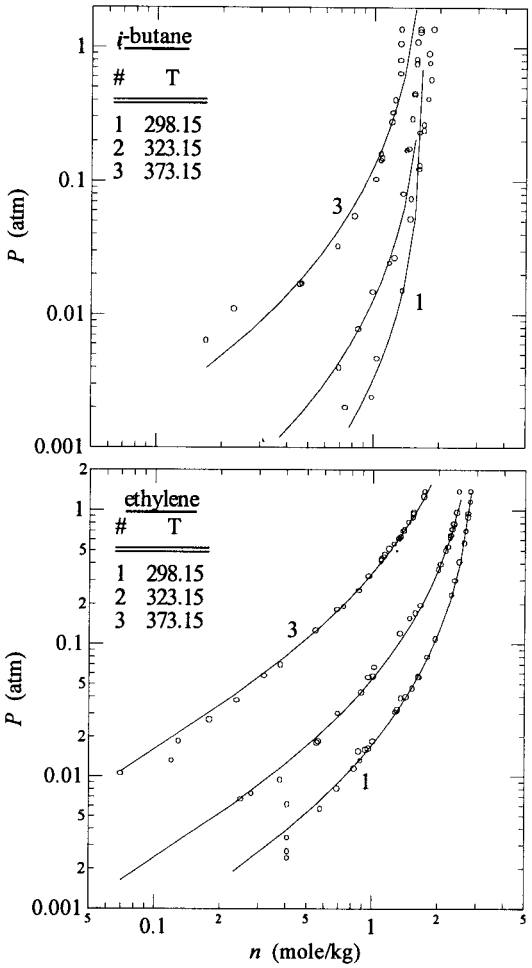

Figure 1. Correlated (HFG) (lines) and experimental (symbols) single component adsorption isotherms on 13X molecular sieve.[36−38]

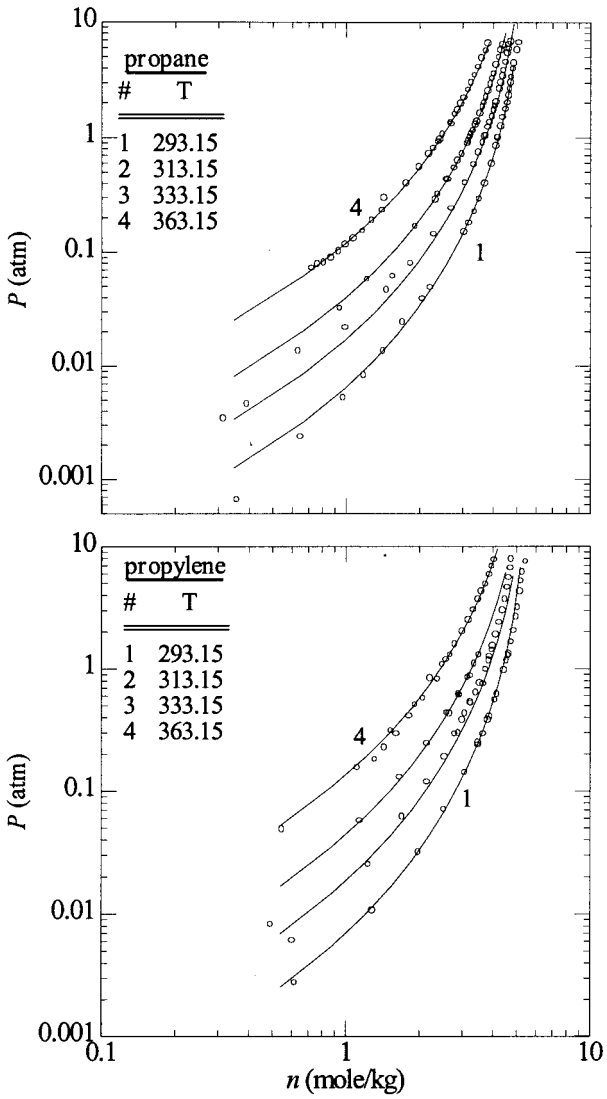

Figure 2. Correlated (HFG) (lines) and experimental (symbols) single component adsorption isotherms on Nuxite-AL activated carbon.[39,40]

a is given by

$$a(T,N_s,N_1,...,N_M) = \exp\left(\frac{-W(N_s,N_1,...,N_M) + \sum_{k=1}^{M} N_k(-U_0)_k}{\kappa T}\right)\prod_{k=1}^{M}[J_k^a(T)]^{N_k} \quad (18)$$

where J_k^a is the partition function for the internal degrees of freedom of a molecule k in the adsorbed phase, U_0 is the energy potential minimum, and W is the Bragg−Williams approximation for the lateral interactions between the neighboring molecules in the adsorbed phase and is estimated from[33,34]

$$W(N_s,N_1,...,N_M) = \sum_{k=1}^{M}\sum_{l=1}^{M}[\bar{N}_{k,l}(N_s,N_k,N_l) \times \omega_{k,l}] \quad (19)$$

$\omega_{k,l}$ is the adsorbate−adsorbate lateral interaction energy between molecules l and k ($w_{k,l} = w_{l,k}$, and $w_{k,k} = w_k$ of single component k), and $\bar{N}_{k,l}$ is the average number of adjacent site pairs occupied by molecules k and l, and is expressed as

$$\bar{N}_{k,l}(N_s,N_k,N_l) = \frac{z}{2}\left(\frac{N_k N_l}{N_s}\right) \quad (20)$$

where z is the total number of nearest neighbors (e.g., $z = 4$ for a square lattice) and the factor $^1/_2$ is introduced to correct for double counting the same pairs. Substituting eqs 19 and 20 into eq 18 gives

$$\ln a = \frac{-z}{2N_s\kappa T}\left(\sum_{k=1}^{M}\sum_{l=1}^{M} N_k N_l \omega_{k,l}\right) + \sum_{k=1}^{M}\left(N_k\left[\frac{(-U_0)_k}{\kappa T} + \ln J_k^a\right]\right) \quad (21)$$

Therefore, the adsorbed phase chemical potential for

(33) Clark, A. *The Theory of Adsorption and Catalysis*; Academic Press: New York, 1970.

(34) Davis, H. T. *Statistical Mechanics of Phases, Interfaces, and Thin Films*; VCH Publishers: New York, 1996.

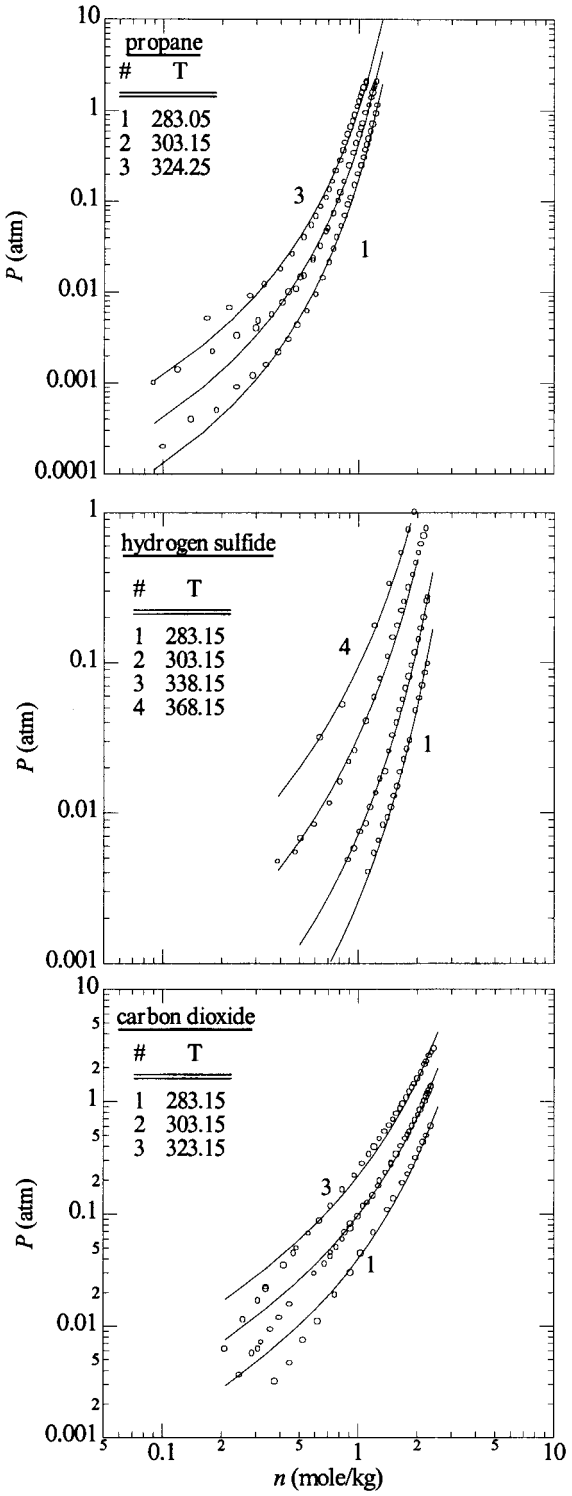

Figure 3. Correlated (HFG) (lines) and experimental (symbols) single component adsorption isotherms on H. mordenite zeolite.[12]

component i becomes

$$\lambda_i^a = \exp\left(\frac{\mu_i^a}{\kappa T}\right) = \exp\left(-\left[\frac{\partial \ln Q}{\partial N_i}\right]_{T,N_s,N_j\neq N_i}\right) = \exp\left(-\left[\frac{\partial(\ln g + \ln a)}{\partial N_i}\right]_{T,N_s,N_j\neq N_i}\right) \quad (22a)$$

Substituting eqs 17 and 21 into eq 22a gives

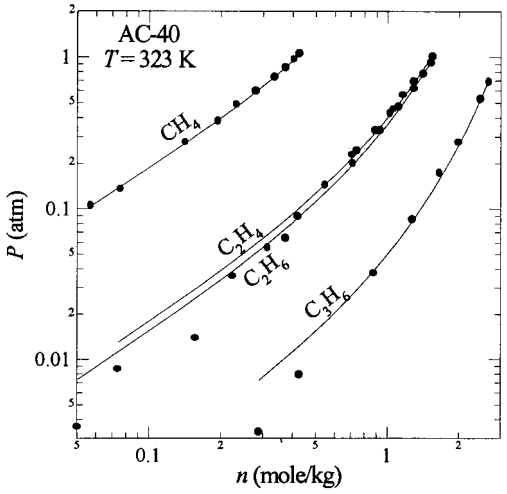

Figure 4. Correlated (HFG) (lines) and experimental (symbols) single component adsorption isotherms on AC-40 activated carbon.[41]

$$\lambda_i^a = \frac{\vartheta_i}{J_i^a(1 - \sum_{k=1}^{M}\vartheta_k)} \exp\left(\frac{1}{\kappa T}[U_{0,i} + z\sum_{k=1}^{M}\vartheta_k\omega_{i,k}]\right) \quad (22b)$$

where $\vartheta_i = N_i/N_s$ is the "local" surface coverage of component i on a homogeneous surface.

At equilibrium, the adsorbed and gas phase chemical potentials of component i are equal. Assuming ideal gas behavior gives the chemical potential of component i in the gas phase mixture as

$$\lambda_i^g = \exp\left(\frac{\mu_i^g}{\kappa T}\right) = \frac{h^3}{\kappa T(2\pi M_i \kappa T)^{3/2} J_i^g(T)} P_i \quad (23)$$

where $J_i^g(T)$ is the partition function for the internal degrees of freedom for molecule i in the gas phase and M_i is the molecular weight of component i. Equating eqs 22b and 23 and solving for the partial pressure of component i gives

$$P_i = \sqrt{\frac{8\pi^3 M_i^3 \kappa^5 T^5}{h^6}}\left(\frac{J_i^g}{J_i^a}\right)\frac{\vartheta_i}{1 - \sum_{k=1}^{M}\vartheta_k} \exp\left(\frac{z}{\kappa T}\sum_{k=1}^{M}\vartheta_k\omega_{i,k}\right) \times \exp\left(\frac{U_{0,i}}{\kappa T}\right) \quad (24)$$

or

$$\beta_i^{(M)} b_i P_i = \frac{\vartheta_i}{1 - \sum_{k=1}^{M}\vartheta_k} \quad (25a)$$

Alternatively,

$$\vartheta_i = \frac{\beta_i^{(M)} b_i P_i}{1 + \sum_{j=1}^{M}\beta_j^{(M)} b_j P_j} \quad (25b)$$

where

$$b_i = \sqrt{\frac{h^6}{8\pi^3 M_i^3 \kappa^5 T^5}}\left(\frac{J_i^a}{J_i^g}\right) = \sqrt{\frac{h^6}{8\pi^3 M_i^3 \kappa^5 T^5}}\left(\frac{J_i^{S,\text{trans}}\ J_i^{S,\text{vib}}\ \exp\left(\frac{\epsilon_i}{RT}\right)}{J_i^g}\right) = b_{0i}\exp\left(\frac{\epsilon_i}{RT}\right) \tag{26}$$

and $\beta_i^{(M)}$ is the lateral interaction term for component i in an M-component mixture, expressed as

$$\beta_i^{(M)} = \exp(-\alpha_i\vartheta_i - \sum_{\substack{k'=1\\k'\neq i}}^{M}\alpha_{i,k'}\vartheta_{k'}) \tag{27}$$

where

$$\alpha_i = \frac{z\omega_i}{\kappa T}, \quad \alpha_{i,k'}(\alpha_i,\alpha_{k'}) = \alpha_{k',i}(\alpha_i,\alpha_{k'}) \tag{28}$$

and ϵ_i is the molar adsorption energy of i ($-U_{0,i}$ times Avogadro's number). Equations 25−28 represent the local FG multicomponent adsorption isotherm on a homogeneous surface. This derivation clearly shows that all of the cross lateral interaction parameters between any pair of components j and k (α_{jk}), not including i, cancel out, in agreement with the final result obtained by the kinetic approach.[31] Therefore, the interaction of only component i with the other $(M-1)$ components is required in eq 27.

Prediction of Multicomponent Adsorption Equilibria on Heterogeneous Surfaces. The FG isotherm is extended here for predicting multicomponent adsorption equilibria on a random heterogeneous surface using only the single component fitting parameters along with the binary fitting parameters, k_{ij}, for each of the binary pairs in the multicomponent mixture. To account for surface heterogeneity, the extended form of the FG isotherm (eqs 25−28) is integrated over a distribution of Henry's law constants on a random heterogeneous surface[16] according to

$$\theta_i = \int_{b_{iL}:}^{b_{iH}}\vartheta_i(b_i,\beta_i^{(M)})\, f(b_i)\, \mathrm{d}b_i \tag{29}$$

where a method referred to as energetic site matching[4,18,35], i.e.,

$$\int_{b_{iL}}^{b_i} f(b_i)\, \mathrm{d}b_i = \int_{b_{jL}}^{b_j} f(b_j)\, \mathrm{d}b_j \tag{30}$$

with

$$f(b_i) = \frac{1}{b_{iH} - b_{iL}} = \frac{1}{\Delta b_i} \tag{31}$$

which leads to

$$\frac{b_i - b_{iL}}{\Delta b_i} = \frac{b_j - b_{jL}}{\Delta b_j} \tag{32}$$

or

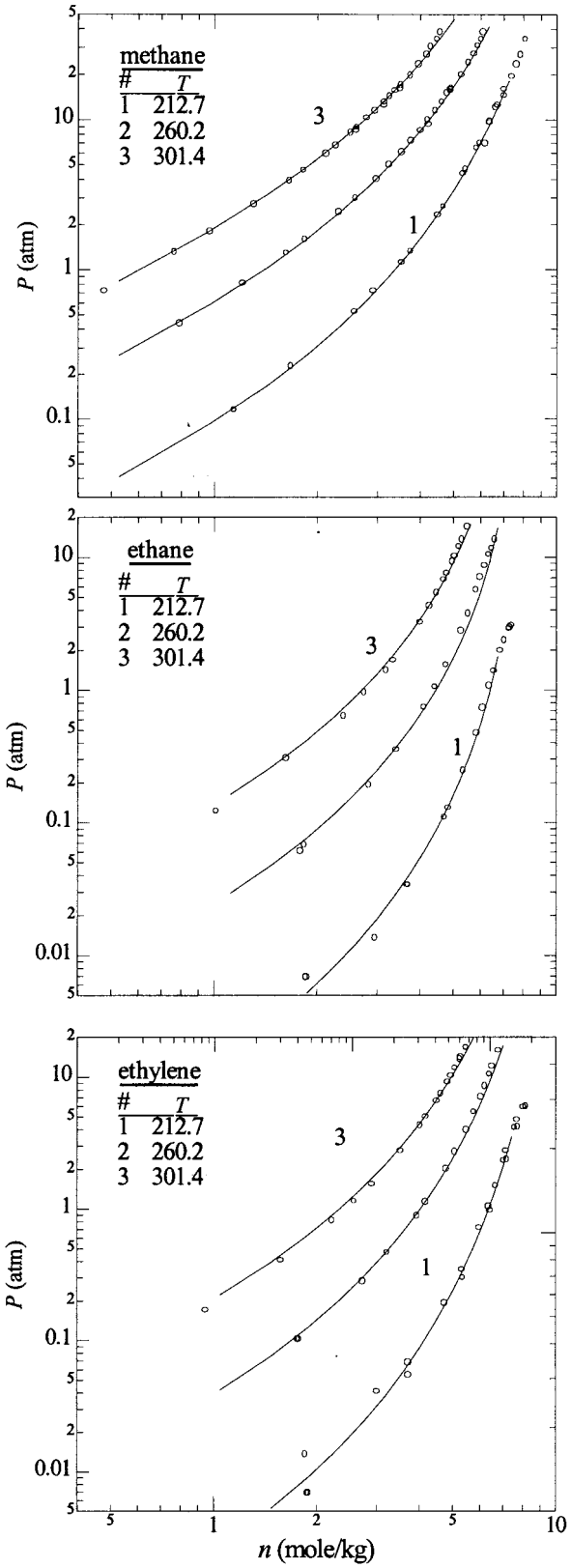

Figure 5. Correlated (HFG) (lines) and experimental (symbols) single component adsorption isotherms on BPL activated carbon.[42]

$$b_j = b_{jL} + \frac{\Delta b_j}{\Delta b_i}(b_i - b_{iL}) \tag{33}$$

is used to simplify eq 29 by providing a functional relationship between $f(b_i)$ and $f(b_j)$.

(35) Hill, T. L. *J. Chem. Phys.* **1949**, *17*, 762.

Table 1. Fitted Single Component Adsorption Isotherm Parameters and ARE[a] Values for the Heterogeneous FG (HFG) and Langmuir (LM)[b] Models

adsorbent	compt	m (mol/kg)	$10^5 b_0$ (atm^{-1})	ϵ/R (K)	$\sqrt{3}\sigma$ (atm^{-1})	$10^{-3}z\omega/\kappa$ (K)	ARE_{HFG} (%)	ARE_{LM} (%)
13X M.S. [ref 36−38]	isobutane	1.675	0.749	5726	20.189	0.639	8.25	9.24
		{1.616}	{0.258}	{5762}				
	C_2H_4	3.035	1.019	4591	0.002	0.502	4.64	11.12
		{2.695}	{1.156}	{4416}				
Nuxite-AL [refs 39, 40]	C_3H_8	5.296	0.949	4643	0.153	1.070	3.46	13.74
		{4.429}	{1.334}	{4168}				
	C_3H_6	5.508	0.632	4710	0.153	1.005	4.59	12.45
		{4.714}	{2.925}	{3831}				
H.M. zeolite [ref 12]	C_3H_8	1.662	1.005	5142	2.024	2.130	12.56	14.68
		{1.056}	{1.061}	{4711}				
	CO_2	5.439	0.763	4147	1.823	1.724	11.21	18.10
		{2.430}	{0.097}	{4793}				
	H_2S	3.352	2.921	4893	5.756	1.639	3.64	9.04
		{2.120}	{30.50}	{3855}				
AC-40 [ref 41] (T = 323 K)	CH4	59.565	9.466×10^2	0	0.086	0.050[c]	1.00	1.29
		{1.443}	{4.083×10^4}	{0}				
	C_2H_6	5.606	1.276×10^5	0	1.273	1.246	13.28	16.44
		{2.130}	{2.544×10^5}	{0}				
	C_2H_4	5.715	1.074×10^5	0	0.939	1.208	7.17	10.22
		{2.136}	{2.295×10^5}	{0}				
	C_3H_6	8.702	6.058×10^5	0	6.033	2.250	12.96	19.94
		{2.963}	{9.168×10^5}	{0}				
BPLA.C. [ref 42]	CH_4	10.704	4.362	2225	0.039	0.808	1.59	9.65
		{7.368}	{9.523}	{1918}				
	C_2H_6	7.474	2.647	3331	1.396	0.818	5.01	11.76
		{6.379}	{1.571}	{3175}				
	C_2H_4	9.023	1.627	3289	0.428	1.068	5.04	13.92
		{6.948}	{1.867}	{2948}				

[a] $ARE = 100\% \left(\sum_{i=1}^{N_P} |n_i^{exp} - n_i^{calc}|/n_i^{exp}\right)/N_P$; N_P is the total number of experimental points. [b] Values in curly brackets "{ }" are the LM fitting parameters. [c] This value was chosen as the minimum allowable value for lateral interactions in order to avoid negative and zero results, i.e., in order to apply eq 7.

The lateral interaction term, $\beta_i^{(M)}$, because of the random heterogeneous surface assumption, depends on the overall heterogeneous surface coverage, θ_i, not on the local homogeneous surface coverage, ϑ_i,[16,17,35] i.e.,

$$\beta_i^{(M)} = \exp\left(-\alpha_i\theta_i - \sum_{\substack{k'=1 \\ k'\neq i}}^{M} \alpha_{i,k'}\theta_{k'}\right) \tag{34}$$

Inserting eqs 33 and 34 into eqs 29 and 31, carrying out the integration and simplifying give

$$\theta_i = \frac{n_i}{m_i} = \frac{\sigma_i\beta_i^{(M)}P_i}{\sum_{j=1}^{M}\sigma_j\beta_j^{(M)}P_j}\left(1 + \frac{1 + \sum_{j=1}^{M}(b_j - b_i\sigma_j/\sigma_i)\beta_j^{(M)}P_j}{2\sqrt{3}\sum_{j=1}^{M}\sigma_j\beta_j^{(M)}P_j} \times \ln\left[\frac{1 + \sum_{j=1}^{M}(b_j - \sqrt{3}\sigma_j)\beta_j^{(M)}P_j}{1 + \sum_{j=1}^{M}(b_j + \sqrt{3}\sigma_j)\beta_j^{(M)}P_j}\right]\right) \tag{35}$$

where the β's are calculated as shown in eq 34 with the binary fitting parameter k_{ij} optimized from the corresponding experimental binary adsorption equilibria. All of the other parameters are obtained from fitting the single component adsorption isotherms to eqs 1−3. Therefore, eq 35 constitutes a predictive model that describes the adsorption of a laterally interacting multicomponent gas mixture on a random heterogeneous surface. Again, in the limits of σ_j and ω_j (j = 1, ..., M) all approaching zero, eq 35 reduces to the familiar mixed LM (MLM) model, which is given by

$$\theta_i = \frac{n_i}{m_i} = \frac{b_iP_i}{1 + \sum_{j=1}^{M} b_jP_j} \tag{36}$$

Results and Discussion

Correlation of Single Component Adsorption Isotherms. Equations 1−3 and the other single component forms of the LRC, 2DF, and LM models were correlated with single component adsorption equilibria on 13X molecular sieve,[36−38] Nuxite-AL activated carbon,[39,40] H. mordenite zeolite,[12] AC-40 activated carbon,[41] and BPL activated carbon.[42] The fitting parameters in each of these models were optimized to the experimental data simultaneously at all temperatures using the least sum square error (LSSE) method in the amount adsorbed. The experimental data and the optimized correlations for the five-parameter HFG model are plotted in Figures 1−5. The regression parameters for each of the HFG and three-parameter LM models and the five-parameter LRC and four-parameter 2DF models are given in Tables 1 and 2, respectively, along with the corresponding average relative errors (AREs) in the amount adsorbed. In almost all cases, the AREs from the HFG model were considerably less than those from the LM model, as expected because of the additional fitting parameters. The LRC and 2DF models

(36) Danner, R. P.; Choi, E. C. *Ind. Eng. Chem. Fundam.* **1978**, *17*, 248.
(37) Hyun, S. H.; Danner, R. P. *J. Chem. Eng. Data* **1982**, *27*, 196.
(38) Kaul, B. K. *Ind. Eng. Chem. Res.* **1987**, *26*, 928.
(39) Szepesy, L.; Illés, V. *Acta Chim. Hung. Tomus.* **1963**, *35*, 37.
(40) Szepesy, L.; Illés, V. *Acta Chim. Hung. Tomus.* **1963**, *35*, 53.
(41) Costa, E.; Calleja, G.; Marro'n, C.; Jiménez, A.; Pau, J. *J. Chem. Eng. Data* **1989**, *34*, 156.
(42) Reich, R.; Ziegler, W. T.; Rogers, K. A. *Ind. Eng. Chem. Process Des. Dev.* **1980**, *19*, 336.

Table 2. Fitted Single Component Adsorption Isotherm Parameters and ARE[a] Values for the Loading Ratio Correlation (LRC) and Two-Dimensional Fluid (2DF) Isotherm Models

adsorbent	compt	m (mol/kg)	k_0	k_1 (K)	B_0	B_1 (K)	q_0 (mol/kg)	ln A_0	γ	ϵ_0/κ (K)	ν/κ^b (K)	ARE_{LRC} (%)	ARE_{2DF} (%)
13X M.S. [refs 36−38]	isobutane	1.6793	−12.267	5471	1.639	46.308	3.345	−11.15	1.707	2138	1584	7.82	10.85
	C_2H_4	3.108	−11.504	4319	0.961	136.320	5.246	−10.59	0.357	3134	1079	3.61	4.49
Nuxite-AL [refs 39, 40]	C3H8	5.505	−11.644	4078	1.233	188.998	8.910	−10.17	0.814	2263	1138	2.02	2.14
	C_3H_6	5.819	−11.921	4113	1.939	−33.440	10.220	−10.38	1.590	1601	1435	2.62	5.17
H.M. zeolite [ref 12]	C_3H_8	1.402	−11.134	4241	1.755	115.017	2.292	−9.80	1.052	2149	1138	7.27	9.77
	CO_2	5.197	−11.300	3227	−0.263	708.417	8.146	−10.59	1.226	1638	937	1.37	2.73
	H_2S	3.577	−10.662	4042	0.633	540.215	5.094	−8.56	1.486	1679	1445	2.04	3.78
AC-40 [ref 41] (T = 323 K)	CH_4	1.266	−0.687	0	0.966	0	2.897	−1.62	0.193	0	713	1.10	1.29
	C_2H_6	4.711	−1.043	0	1.548	0	4.360	2.27	242.6	0	1035	3.71	19.93
	C_2H_4	4.264	−0.807	0	1.441	0	4.357	2.69	703.4	0	1079	2.30	14.34
	C_3H_6	6.233	−0.165	0	1.930	0	5.712	4.04	1156	0	1435	0.91	27.75
BPLA.C. [ref 42]	CH_4	10.010	−9.998	1867	1.076	137.148	17.794	−8.76	2.196	592	713	2.65	2.48
	C_2H_6	8.146	−11.222	2987	1.978	7.763	13.612	−9.98	1.584	1206	1035	3.01	4.29
	C_2H_4	9.729	−11.343	2739	1.540	159.805	15.543	−9.60	2.348	843	1076	2.98	3.89

[a] ARE is defined as in Table 1. [b] ν/κ is estimated from the Lennard-Jones potential parameters as shown in ref 26.

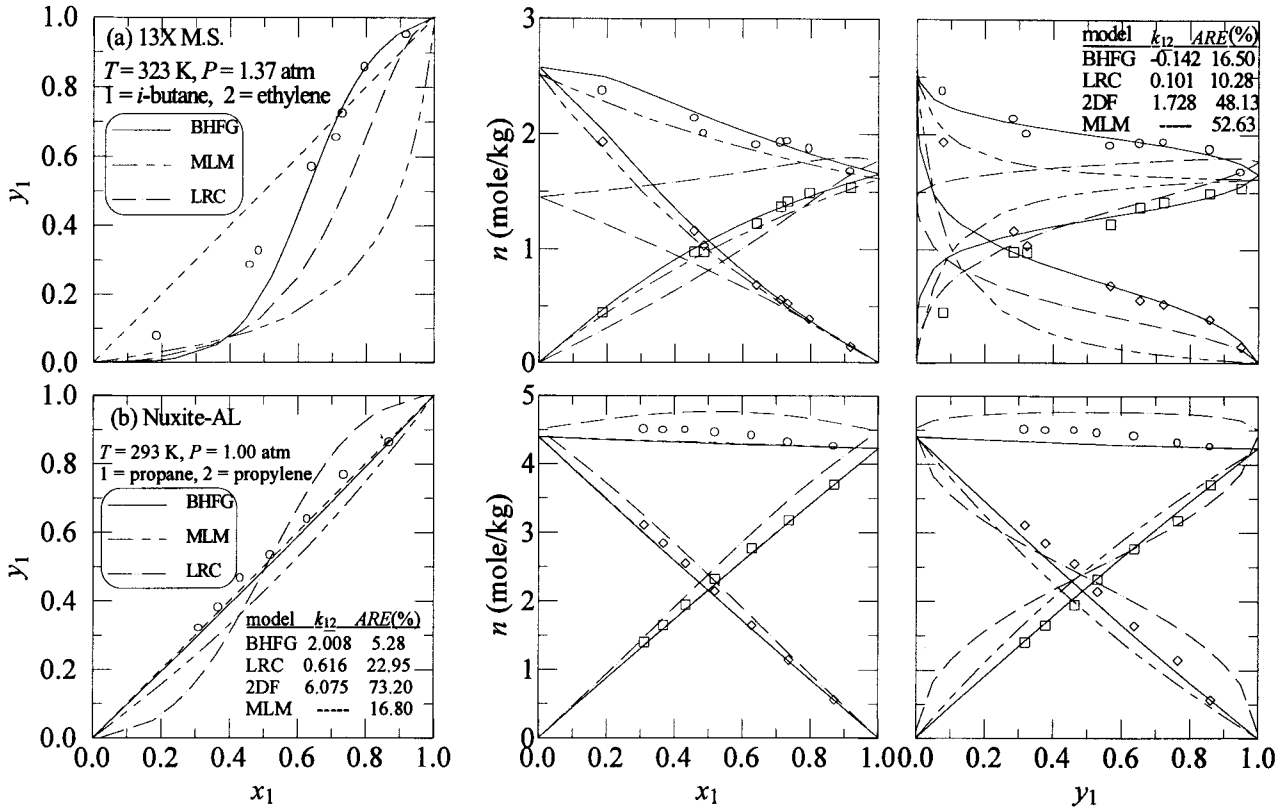

Figure 6. Correlated (BHFG, solid lines; LRC, dashed lines), predicted (MLM) (dash−dot−dot lines), and experimental (symbols) binary adsorption equilibria on (a) 13X molecular sieve[36−38] and (b) Nuxite-AL activated carbon.[43] Each row represents one binary system plotted in different coordinates, and x_i and y_i are the mole fractions of component i in the adsorbed and gas phases, respectively.

gave the best results in correlating the single component adsorption equilibria; therefore, they are expected to be strong competitors for the new model in correlating binary adsorption equilibria. The single component parameters from these models are used below for the correlation (HFG, LRC, and 2DF) or prediction (LM) of complex binary adsorption equilibria and for the correlation (LRC) and prediction (HFG, 2DF and LM) of multicomponent adsorption equilibria.

Correlation of Complex Binary Adsorption Equilibria. The ability of eq 5, which is referred to as the binary HFG (BHFG) model, to correlate complex binary adsorption equilibria, because of the remarkable flexibility introduced by the binary fitting parameter, k_{12}, is demonstrated here by fitting sample binary systems that exhibit azeotropic behavior and/or sigmoidal-shaped $x-y$ diagrams. As explained previously, these are two very severe nonidealities that only a few models in the literature can correlate efficiently while maintaining their ease of application. Figures 6−8 and Tables 3 and 4 show correlations with eq 5 for binary adsorption equilibria on 13X molecular sieve,[36−38] Nuxite-AL activated carbon,[43]

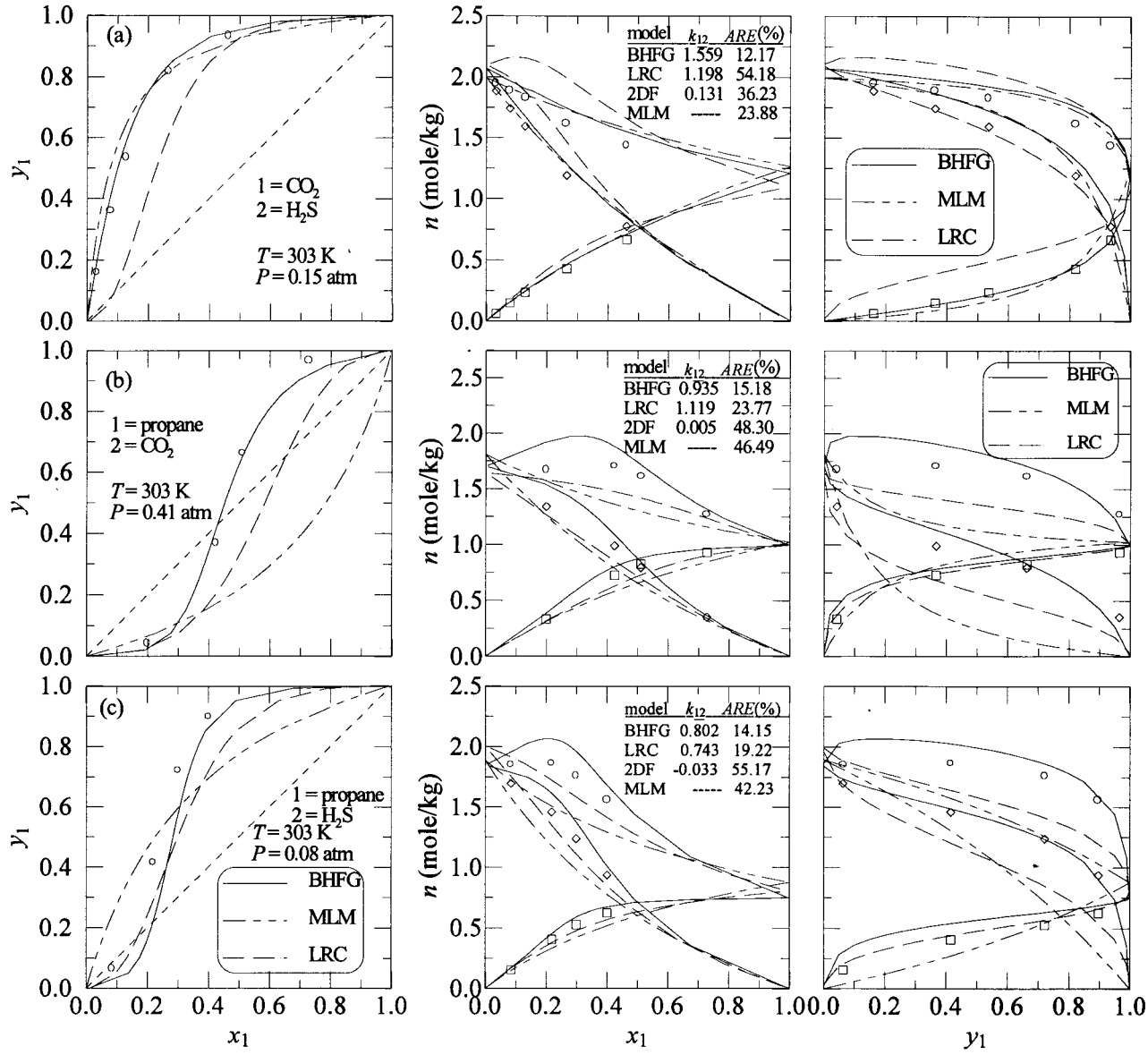

Figure 7. Correlated (BHFG, solid lines; LRC, dashed lines), predicted (MLM) (dash−dot−dot lines), and experimental (symbols) binary adsorption equilibria on H mordenite zeolite.[12] Each row represents one binary system plotted in different coordinates.

Table 3. Optimized k_{12} Values from the Binary HFG (BHFG), LRC, and 2DF Models, and ARE Values from the BHFG, LRC, 2DF, and Multicomponent Langmuir (MLM) Models for Binary Adsorption Equilibria on AC-40 Activated Carbon[41] at 323 K and 0.10 atm

	$k_{12} = k_{21}$			ARE (%)			
binary pair	BHFG	LRC	2DF	BHFG	LRC	2DF	MLM
$CH_4 + C_2H_4$	6.256	1.054	0.045	16.58	18.16	33.26	28.66
$CH_4 + C_2H_6$	13.72	1.467	−0.040	33.54	26.17	55.37	52.13
$C_2H_4 + C_2H_6$	2.066	1.196	−0.310	11.18	19.60	18.99	13.48
$C_2H_6 + C_3H_6$	2.287	1.422	0.381	18.57	31.43	30.57	29.00
$C_2H_4 + C_3H_6$	2.906	1.375	0.008	29.97	35.33	49.98	46.86

H. mordenite zeolite,[12] AC-40 activated carbon,[41] and BPL activated carbon.[42] These figures and tables also show the corresponding correlations and predictions from the LRC, 2DF, and MLM models, respectively. Note that only the three optimized single component isotherm parameters ϵ_i, $b_{0,i}$, and m_i were used in the MLM. Since the BHFG and 2DF models are implicit in the amount adsorbed, an initial assumption of the amounts adsorbed must be provided into the objective function

$$F = \sum_{j=1}^{N_P}\left(\sum_{i=1}^{M} w|n_i^a - n_i^{\text{calc}}| + |n_i^{\text{calc}} - n_i^{\text{exp}}|\right)_j \qquad (37)$$

where N_P is the total number of data points and $M = 2$. w is a weighing factor that was set to 1 for the BHFG model and 10−100 for the 2DF model. The superscripts "a," "calc", and "exp" indicate assumed, calculated, and experimental amounts adsorbed, respectively. The calculated amounts adsorbed were estimated according to eq 5, and eqs 8 and 11 for the BHFG and 2DF models, respectively. In addition to k_{12}, it was necessary to iterate on the assumed amount adsorbed of each component on each of the four patches according to eq 8 to optimize the 2DF model. In contrast, in addition to k_{12}, the assumed absolute amounts adsorbed of each component were used as the manipulated variables for the BHFG model. Therefore, the 2DF model required many more iterations and a higher value of w than the BHFG model to achieve convergence. Since the LRC model is explicit in the amount adsorbed, the first term of eq 37 was eliminated and k_{12}

(43) Szepesy, L.; Illés, V. *Acta Chim. Hung. Tomus.* **1963**, *35*, 245.

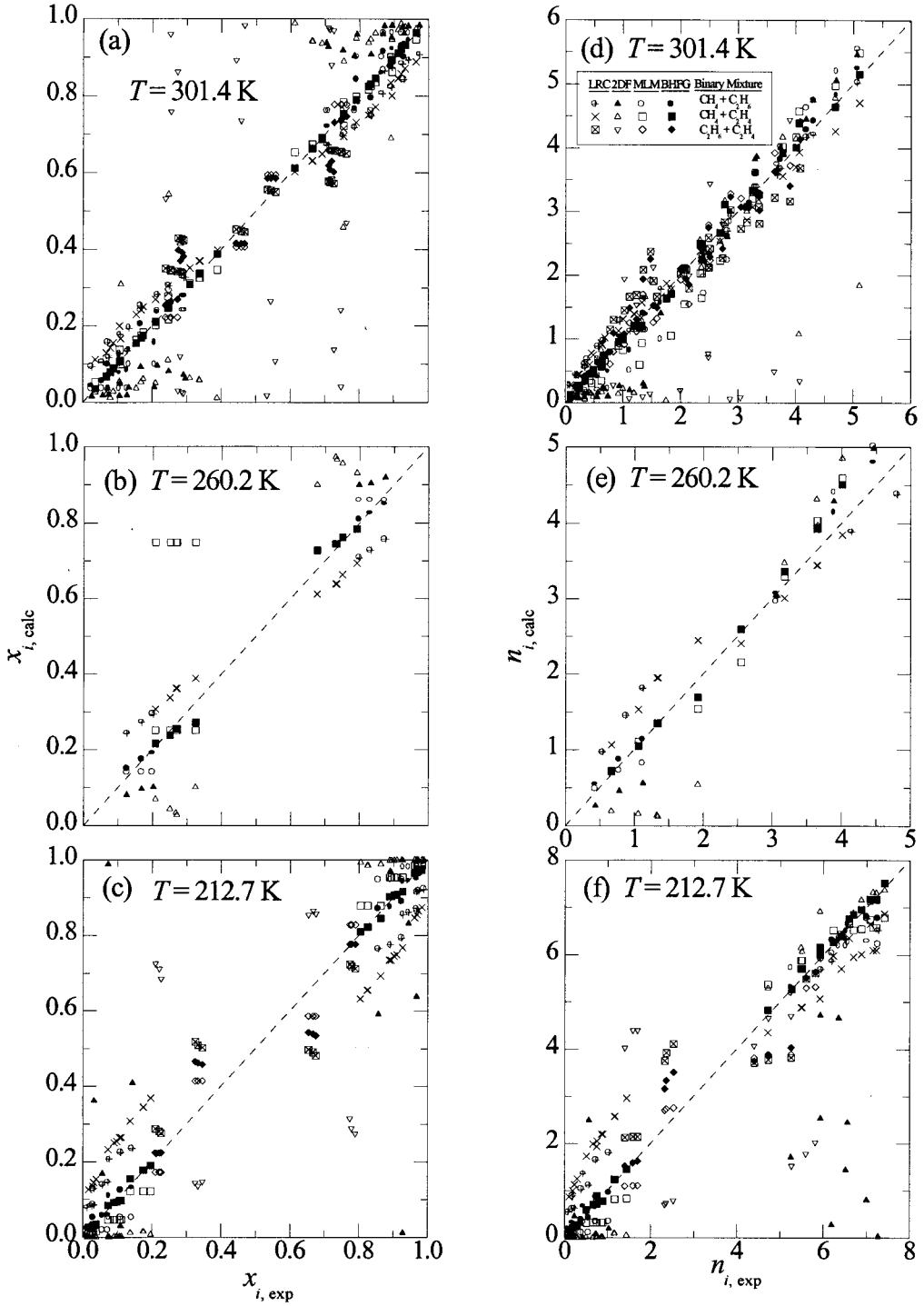

Figure 8. Correlated (BHFG, LRC, and 2DF) and predicted (MLM) vs experimental binary (a−c) adsorbed phase compositions and (d−f) component amounts adsorbed on BPL activated carbon.[42]

was treated as the only manipulated variable. The goodness of the correlations with the BHFG, LRC, and 2DF models and predictions with the MLM model was estimated using the binary/multicomponent average relative error in the amount adsorbed, which is calculated from

$$\mathrm{ARE}(\%) = \frac{100\%}{M \times N_P} \sum_{l=1}^{N_P} \left[\sum_{j=1}^{M} \frac{|n_j^{\mathrm{exp}} - n_j^{\mathrm{calc}}|}{n_j^{\mathrm{exp}}} \right]_l \qquad (38)$$

with the superscript "calc" indicating either correlated or predicted amounts adsorbed. The optimum k_{12} values and the corresponding AREs for the three models are shown for each binary system in Figures 6 and 7 and Tables 3 and 4.

Figure 6 shows two examples of complex binary adsorption equilibria that exhibit in one case (Figure 6a) a single azeotropic composition with a sigmoidal-shaped $x-y$ diagram and in the other case (Figure 6b) a wide range of azeotropic compositions, i.e., no selectivity over the entire composition range. Because of the binary fitting parameter, k_{12}, along with corrections for adsorbate−adsorbate lateral interactions and surface heterogeneity, the BHFG model provided an excellent description of the $x-y$ diagram in both cases; the MLM model failed in both

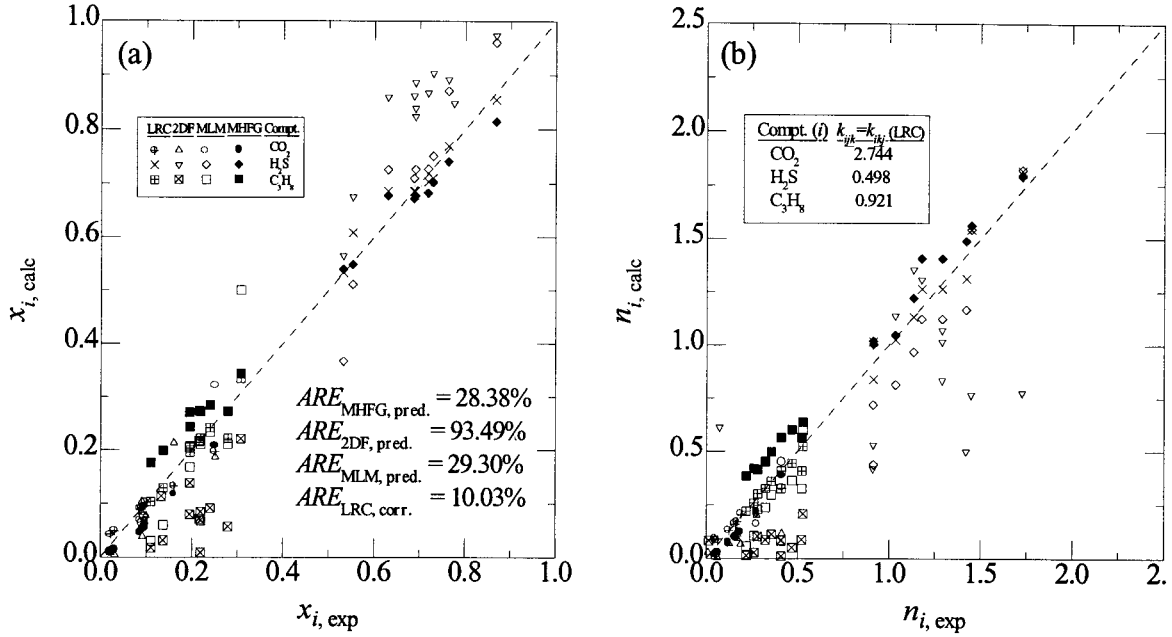

Figure 9. Predicted (MHFG, 2DF, and MLM) and correlated (LRC) vs experimental ternary (a) adsorbed phase compositions and (b) component amounts adsorbed on H mordenite zeolite.[12]

Table 4. Optimized k_{12} Values from the BHFG, LRC, and 2DF Model, and ARE Values from the BHFG, LRC, 2DF, and MLM Models for Binary Adsorption Equilibria on BPL Activated Carbon[42]

		$k_{12} = k_{21}$			ARE (%)			
T (K)	P (atm)	BHFG	LRC	2DF	BHFG	LRC	2DF	MLM
			$CH_4 + C_2H_6$					
301.4	1.3−19.8	1.239	0.950	3.318	11.36	33.61	39.24	19.96
260.2	1.2−9.3	1.489	0.834	0.661	8.50	45.14	25.46	12.54
212.7	1.3−8.6	1.530	0.682	139.6	16.73	114.98	87.88	32.82
			$CH_4 + C_2H_4$					
301.4	1.2−20.0	1.417	1.153	7.638	6.27	30.53	40.10	15.61
260.2	1.4−13.9	1.649	1.182	4.637	5.62	24.80	46.74	8.95
212.7	1.3−10.3	1.711	0.883	10.13	7.47	130.55	51.13	24.11
			$C_2H_6 + C_2H_4$					
301.4	1.4−19.6	1.660	1.490	15.70	12.68	22.85	53.31	12.91
212.7	1.4−4.0	1.784	0.647	3.629	15.78	30.92	79.60	16.67

cases, especially in the first case. Also, the BHFG model provided an almost exact description of both of the $n-x$ and $n-y$ diagrams. Although the ability of the MLM model to predict the $n-x$ diagram was always satisfactory, it tended to underestimate the experimental values, especially in Figure 6a. Also, it failed to predict the plateau of the total amount adsorbed at low values of x_1, where the BHFG model did not. The LRC model gave satisfactory results in correlating the system in Figure 6a, but failed in correlating the composition of the binary system in Figure 6b. Apparently, the binary interaction parameter k_{12} (or η) in the LRC model is not as flexible as it is in the BHFG model. The 2DF model (only its k_{12} and ARE values are shown in Figures 6 and 7, without the curves) was capable of correlating the adsorption equilibria, but only within very narrow ranges of composition, and in most cases it was inferior even to the LRC model. It also showed a lack of flexibility to give the same shape of the $x-y$ diagrams as the experimental adsorption equilibria and very often seriously underestimated the amounts adsorbed. As a result of these differences between the three models in describing such complex binary behavior, the AREs were much lower for the BHFG model compared to the MLM and 2DF models, and lower than or equivalent to those of the LRC model.

Figure 7 shows three pairs of additional binary systems on H. mordenite zeolite. These three pairs were needed to test the ability of the multicomponent HFG (MHFG) model to predict ternary adsorption equilibria of propane, carbon dioxide, and hydrogen sulfide on H. mordenite zeolite from single component and binary data, as shown in the following section. The CO_2-H_2S binary system shown in Figure 7a did not exhibit any complex binary behavior; therefore, the MLM model predictions and LRC and 2DF model correlations were not much worse than the BHFG correlations. However, the LRC model had a tendency to falsely provide a sigmoidal shaped $x-y$ diagram, and the 2DF model required many more iterations than the BHFG model and, as noticed before in Figure 6, it was capable of providing multiple solutions. When complex azeotropic behavior and/or sigmoidal-shaped $x-y$ diagrams were considered, as shown in Figure 7b and Figure 7c for the $C_3H_8-CO_2$ and $C_3H_8-H_2S$ systems, respectively, the MLM model failed in predicting the actual $x-y$ diagrams. Also, as noticed before in Figure 6, the BHFG model gave a much better description of the $n-x$ and $n-y$ diagrams than the MLM, LRC, and 2DF models. This is noticeable mostly when correlating the plateau in the total amount adsorbed as shown in the $n-x$ diagram in Figure 7c. The AREs from the BHFG model, in both of these cases, were again much lower than those from the MLM, LRC, and 2DF models. The effect of these improved correlations on the predictions of multicomponent adsorption equilibria is further discussed in the following section. Table 3 also shows the binary fitting parameters for another set of binary mixtures adsorbed on AC-40 activated carbon[41] that are used later for predicting ternary adsorption equilibria. Even though these mixtures did not always exhibit complex behavior, the AREs obtained from the BHFG model were in almost all cases significantly less than those from the MLM, LRC, and 2DF models.

The last case discussed in this section is for binary adsorption equilibria on BPL activated carbon. The challenging consideration in this case was that the experimental binary adsorption equilibria were measured over a relatively wide range of total pressure and fixed composition planes at each temperature. Therefore, it was

necessary to assume that k_{12} depended only on T and the selected pair of adsorbates, regardless of the pressure. A comparison between the experimental and calculated adsorbed phase compositions and amounts adsorbed at the experimental values of the partial pressures is shown in Figure 8 for each of the BHFG, LRC, 2DF, and MLM models. The optimum k_{12}'s and the corresponding AREs from both models are shown in Table 4. The AREs from the BHFG model were still in most cases better than those from the MLM and 2DF models. Moreover, the k_{12}'s from the BHFG model showed a more consistent trend of variation with temperature than the LRC and 2DF models.

Prediction of Multicomponent Adsorption Equilibria. The ability of the MHFG model to predict multicomponent adsorption equilibria according to eq 35 was also examined and compared to the MLM (eq 36), LRC, and 2DF models. The ternary adsorption equilibria on H. mordenite zeolite[12] and BPL activated carbon were the only data available for this purpose because k_{12}'s from all the binary pairs were needed in the MHFG and 2DF models. Note that since only single component isotherm parameters and the k_{12}'s obtained from all of the binary pairs were used in the MHFG and 2DF models, they were completely predictive for multicomponent adsorption equilibria. However, the interaction parameters for the multicomponent form of the LRC model cannot be estimated from those of the corresponding binary mixtures. Therefore, it had to be applied to the multicomponent adsorption equilibria in a correlative mode. The correlated multicomponent interaction parameters for the LRC model are shown in Figures 9−11.

Figure 9 shows a comparison between the experimental and predicted (MHFG, 2DF, and MLM models) and correlated (LRC model) adsorbed phase compositions and amounts adsorbed on H. mordenite zeolite for each component in the ternary mixture $CH_4-C_2H_6-C_2H_4$. The partial pressures for each component in the mixture were fixed at the experimental values, and the k_{12}'s given in Figure 7 were used for each binary system. The predicted compositions and amounts adsorbed using the MHFG model were in most cases aligned with the equality line. Again, the 2DF model resulted in a serious underestimation of the predicted amounts adsorbed for this system. Similar results were also obtained from predicting the multicomponent adsorption equilibria for the $CH_4-C_2H_6-C_2H_4$ system on AC-40 activated carbon, as shown in Figure 10. In both cases, the predictions from the 2DF and MLM models and most of the correlations from the LRC model were much farther from the experimental values, exhibiting ARE values that were considerably higher than those from the MHFG. Clearly, the MHFG model was also capable of predicting multicomponent adsorption equilibria for fairly nonideal systems.

Figure 11 shows the same comparison but for ternary adsorption equilibria of $CH_4-C_2H_6-C_2H_4$ on BPL activated carbon. For this system, all the models resulted in almost the same predictions. It was surprising that the use of a binary fitting parameter did not satisfactorily improve the predictions, especially since for two of the three binary pairs the BHFG model out-performed the MLM model, as shown in Table 4. Nevertheless, the predictions from the BHFG model were equivalent to or better than those obtained with the other three models. Clearly, additional multicomponent adsorption data are needed to further test the MHFG model.

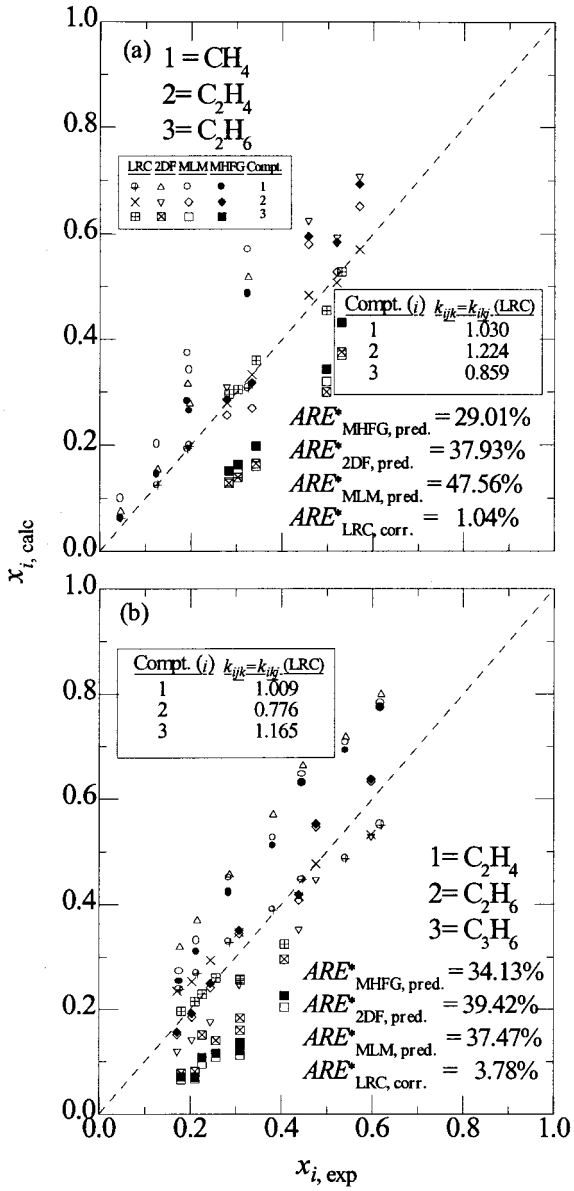

Figure 10. Predicted (MHFG, 2DF, and MLM) and correlated (LRC) versus experimental ternary adsorbed phase compositions on AC-40 activated carbon.[41]

Conclusions

The model developed in part 1 of this series was correlated successfully with very complex binary adsorption equilibria using only single component isotherm parameters and one binary fitting parameter. A remarkable accuracy was achieved for different complex binary mixtures, including those that exhibited adsorption azeotropes and sigmoidal-shaped $x-y$ diagrams. The average relative error (ARE) in the component amounts adsorbed were in most cases substantially lower than those obtained from the popular multicomponent Langmuir model (MLM), and similar two-dimensional fluid model (2DF) and loading ratio correlation (LRC) model that also utilized binary fitting parameters. This new model was also extended successfully for the prediction of multicomponent adsorption equilibria on a heterogeneous surface with a uniform distribution of Henry's law constant using only single component adsorption isotherm parameters, along with a binary fitting parameter (k_{12}) obtained from each of the binary pairs in the multicomponent mixture. Very good predictions of ternary adsorption equilibria were obtained; in most cases, the AREs were much lower than those obtained from the MLM, LRC, and 2DF models. Moreover,

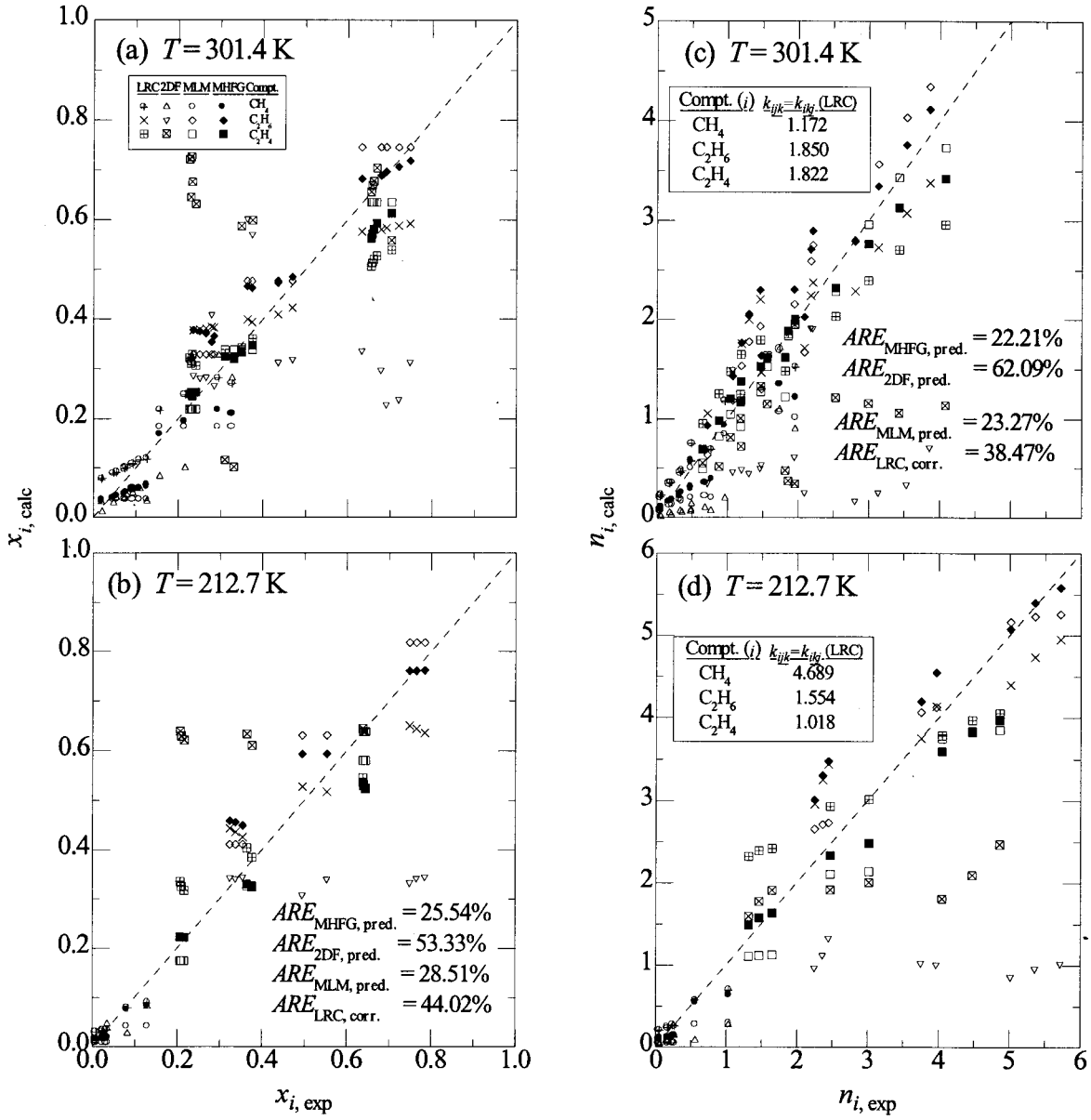

Figure 11. Predicted (MHFG, 2DF, and MLM) and correlated (LRC) versus experimental ternary (a, b) adsorbed phase compositions and (c, d) component amounts adsorbed on BPL activated carbon.[42]

this new model is easy to use, as it requires very few iterations to solve the implicit set of coupled algebraic equations. It should thus find considerable use in correlating both ideal and complex binary adsorption equilibria and in predicting multicomponent adsorption equilibria from correlated single component and binary data. Very few models in the literature can predict complex, multicomponent adsorption equilibria while still maintaining their ease of application.

Acknowledgment. We gratefully acknowledge financial support from the Westvaco Charleston Research Center and the Separations Research Program at the University of Texas at Austin.

LA990242G